



HAL
open science

Photofragmentation of BF₃ on B and F K-shell excitation by partial ion yield spectroscopy

Renaud Guillemin, Wayne C Stolte, Maria Novella Piancastelli, Dennis W Lindle

► **To cite this version:**

Renaud Guillemin, Wayne C Stolte, Maria Novella Piancastelli, Dennis W Lindle. Photofragmentation of BF₃ on B and F K-shell excitation by partial ion yield spectroscopy. *Journal of Physics B: Atomic, Molecular and Optical Physics*, 2010, 43 (21), pp.215205. 10.1088/0953-4075/43/21/215205. hal-00569860

HAL Id: hal-00569860

<https://hal.science/hal-00569860>

Submitted on 25 Feb 2011

HAL is a multi-disciplinary open access archive for the deposit and dissemination of scientific research documents, whether they are published or not. The documents may come from teaching and research institutions in France or abroad, or from public or private research centers.

L'archive ouverte pluridisciplinaire **HAL**, est destinée au dépôt et à la diffusion de documents scientifiques de niveau recherche, publiés ou non, émanant des établissements d'enseignement et de recherche français ou étrangers, des laboratoires publics ou privés.

Photofragmentation of BF_3 upon B and F K-shell excitation by partial ion yield spectroscopy

Renaud Guillemin,^{1,2} Wayne C Stolte,³ Maria Novella Piancastelli,⁴ and Dennis W Lindle³

¹ CNRS, UMR 7614, Laboratoire de Chimie Physique Matière et Rayonnement, F-75005 Paris, France

² UPMC, Univ Paris 06, UMR 7614, Laboratoire de Chimie Physique Matière et Rayonnement, F-75005 Paris, France

³ Department of Chemistry, University of Nevada, Las Vegas, NV 89154-4003, USA

⁴ Department of Physics and Astronomy, Uppsala University, PO Box 516, SE-751 20 Uppsala, Sweden

Abstract. The fragmentation of core-excited BF_3 has been studied by means of partial cation and anion yield measurements around the B and F *K* edges. All detectable ionic fragments are reported, and differences among fragments are discussed. The observations confirm earlier findings on the dynamics of molecular fragmentation studied by partial ion yields, notably on the influence of Rydberg excitations on fragmentation, the behavior of anion production near threshold, and the importance of intramolecular rearrangement in the formation of F_2^+ ions.

PACS numbers: 33.80.Gj, 33.80.Eh

1. Introduction

The electronic structure and core excitation and decay dynamics of the highly symmetric planar molecule BF₃ have been studied extensively with several spectroscopies. These studies include B 1s absorption [1, 2, 3], F 1s absorption [1, 4], and electronic decay after resonant B 1s → 2a₂^{''} excitation to the lowest unoccupied molecular orbital [1, 5, 6, 7, 8]. Ionic fragmentation following B 1s → 2a₂^{''} excitation has been investigated by means of various coincidence techniques, such as resonant-Auger-electron-photoion coincidence [9, 10] and photoelectron-photoion-photoion coincidence [11]. Of particular interest in many of these studies, both experimentally [1, 8, 9, 11, 12] and theoretically [13], have been the effects of nuclear motion in this core-excited state.

Subthreshold resonant excitation of a core electron into an empty molecular orbital may result in rearrangement of the entire electronic structure of the molecule. The combined effect of an additional electron in the valence shell, usually in an antibonding orbital, and an additional positive charge in the core may induce geometrical changes depending on several parameters: the character of the resonant state, the core-hole life time of the inner-shell vacancy, and the mass of the involved atoms. In that regard, an interesting situation occurs when the excited state is bound and the final state has a different equilibrium geometry as compared to the ground state. Significant vibrational excitation is then expected to occur in the final ionic state as a consequence of conformational changes between the ground, intermediate, and final states [15, 16]. In BF₃, such a dynamical effect induces strong out-of-plane vibrational excitation in the ion due to the initial excitation from a planar conformation (D_{3h} point group) in the ground state to a pyramidal one (C_{3v} point group) in the 2a₂^{''} excited state upon boron 1s core excitation. This conformational change induces a new effect directly related to the nuclear dynamics in the core-excited state: so-called ‘dynamical Auger emission’ [5]. The molecular deformation from D_{3h} to C_{3v} in the core-excited state of BF₃ has been confirmed experimentally by electron-ion coincidence experiments [9, 11, 12]. For excitation of BF₃ above the ionization threshold, the most energetic ion is F⁺, and it is ejected in the plane of the molecule. In contrast, for B 1s → 2a₂^{''} resonant excitation, the most energetic fragment ion is B⁺, and it is ejected out of the molecular plane. This latter result clearly indicates an out-of-plane displacement of the B atom in the core-excited state, which is caused by quasi-Jahn-Teller coupling between the B 1s → 2a₂^{''} and the B 1s → 3a₁ core-excited states through the a₂^{''} symmetry vibration [13].

Furthermore, the photoabsorption spectra around both the B and F *K* edges are good examples of a system possessing pronounced shape resonances. The B 1s absorption spectrum shows only two prominent resonances, B 1s → 2a₂^{''} below threshold and the B 1s → 4e′ shape resonance above threshold, while the Rydberg series are very weak. Similar features are observed at the F *K* edge. This peculiar intensity distribution can be explained using the usual potential-barrier concept in which the cage of electronegative F atoms forms a potential barrier, and the strong resonance structures

are regarded as excitations of a core electron into unoccupied orbitals localized inside the potential barrier. In this picture, the $4e'$ resonance above threshold is regarded as a shape resonance trapped by this potential barrier [14].

The present work is part of a systematic study we have conducted on about 20 molecules, from small diatomics such as carbon monoxide [17, 18] to larger systems such as formic acid [19]. Here, we complement the work cited above on core photoexcitation of BF₃ with total and partial ion-yield experiments at both the B and F *K* edges. We use the information provided by single-channel measurements such as partial cation and anion yields to clarify certain aspects of the fragmentation dynamics. In general, we find that below the B $1s$ threshold the relative intensities of spectral features related to core-to-Rydberg excitations increase as the fragmentation process is more extended; for the smallest fragments, Rydberg states are much more prominent than for the parent molecular ions. We attribute this result to spectator decay being much more probable following excitation to a diffuse Rydberg orbital, and the fact that most of the final two-hole/one-particle states are expected to be dissociative [20, 21, 22]. In addition, the experimental resolution available allowed us to determine accurately the vibrational spacing related to the B $1s \rightarrow 3p$ Rydberg transition.

In the vicinity of the shape resonance above threshold, unusually high yields of singly charged cations are observed, at variance with the usual finding that doubly charged cations, resulting from normal Auger decay, show the most intense shape-resonant enhancement. This is attributed to a fast fragmentation of the BF₂⁺⁺ fragment, yielding BF⁺ + F⁺, possibly due to a distorted geometry in the doubly charged species. We also observe a slight enhancement due to the shape resonance in the anion yields, and we conclude that the BF₃ molecule can undergo extended fragmentation leading to anions after normal Auger decay occurs, at variance with the behavior of most small molecules, where anions are not produced in the shape-resonance region. We also observe an exponential decay in the anion yield across the F $1s$ ionization threshold, with a characteristic shape due to post-collision interaction (PCI) and electron recapture effects. Furthermore, we observe formation of the F₂⁺ recombination fragment at the F *K* edge and explain it as related to the previously observed out-of-plane nuclear motion of the B atom.

2. Experimental details

The present ion-yield measurements were performed using undulator beamline 8.0.1.3 at the Advanced Light Source (Lawrence Berkeley National Laboratory, Berkeley, CA). The beamline is equipped with three interchangeable spherical gratings with respectively 150, 380, and 925 lines/mm for high resolution and high flux. It provides 10^{11} to 6×10^{15} photons/s in the 80–1400 eV photon-energy range with a maximum resolving power of $E/\Delta E < 8000$. Grating and slit sizes were chosen to achieve 60 meV resolution at 200 eV photon energy (B *K* edge), and 0.3 eV at 600 eV photon energy (F *K* edge), providing sufficient resolution and photon flux (approximately 5×10^{12} photons/s) for a

reasonable anion signal. Contamination by third-order light from the undulator passing through the monochromator accounts for less than 1% of the total photon flux.

Partial cation and anion yields were obtained with a magnetic mass spectrometer described previously [23]. The instrument consists of a 180° magnetic mass spectrometer with a resolution of 1 mass in 50, an electrostatic lens to focus the ions created in the interaction region onto the entrance slit of the spectrometer, and an effusive-jet gas cell containing push and extraction plates to move the ions from the interaction region into the lens. Ions are detected with a channel electron multiplier (CEM) at the exit slit of the spectrometer. The polarities of the lens, magnetic field, and CEM may be switched, allowing measurement of either cations or anions produced by photofragmentation. The working pressure in the target chamber was set to 1×10^{-5} Torr. An analog signal from a capacitance manometer is recorded simultaneously with the ion signal and incident photon flux to monitor target gas pressure for a point-by-point normalization of the recorded spectra. In order to obtain reasonable statistics, most of the spectra presented in this study are the sum of several recordings, separately normalized. BF_3 was obtained commercially from Airgas specialty gases and equipment, with a stated chemical purity of 99.9%.

3. Results and discussion

The BF_3 molecule has a D_{3h} planar geometry in the ground state, and in an independent-particle model its electronic configuration is:

$$\underbrace{(1a'_1)^2(1e')^4}_{\text{F } 1s} \quad \underbrace{(2a'_1)^2}_{\text{B } 1s} \quad \underbrace{(3a'_1)^2(2e')^4}_{\text{Inner valence shells}} \quad \underbrace{(4a'_1)^2(3e')^4(1a''_2)^2(4e')^4(1e'')^4(1a'_2)^2(2a''_2)^0}_{\text{outer valence shells}}.$$

The inner-valence orbital character is mostly F 2s. The next six occupied orbitals are outer valence: $4a'_1$, $3e'$ and $1a''_2$ are bonding; $4e'$ and $1e''$ are slightly bonding, having mostly F 2p character; whereas $1a'_2$ is nonbonding, having pure F 2p character. The lowest unoccupied molecular orbital is $2a''_2$, having B $2p_z$ character, and is nonbonding. The $4e'$ unoccupied orbital has antibonding character and corresponds to the shape resonance. In the following, we will discuss the two K edges separately.

3.1. B K edge

Figure 1 shows the total-ion-yield spectrum obtained as a sum of all detected ions (equivalent to absorption) in the photon-energy range 290-330 eV, in the region of the B 1s ionization threshold at 202.8 eV. The photon-energy calibration is based on the literature assignment [2, 3]. The intense broad band at 195.5 eV corresponds to promotion of the B 1s electron to the lowest unoccupied molecular orbital $2a''_2$. The width of this band (FWHM) is ~ 250 meV, much larger than the expected natural lifetime width of ~ 60 meV. Therefore, this band consists of unresolved vibrational components with

energy spacings smaller than the natural lifetime width of the inner-shell-hole state. The weak band at 198.2 eV corresponds to the B $1s \rightarrow 3sa'_1$ dipole-forbidden transition, which gains intensity from the B $1s \rightarrow 2a''_2$ transition by coupling through the out-of-plane vibrational displacement of a'' symmetry. Vibrational structure is observable in this band. The energy spacing of the two prominent vibrational components is ~ 100 meV and corresponds to the frequency of the breathing mode ν_2 . The two prominent components are assigned to $(\nu_1, 1)$ with $\nu_1 = 0, 1$ [3]. The following peak at 200.35 eV is assigned to the B $1s \rightarrow 3p$ transition, again with resolved vibrational structure. The weaker structure at 201.6 eV corresponds to the B $1s \rightarrow 4p$ excitation. The insert in figure 1 shows an expanded view of the photon-energy region around the B $1s \rightarrow 3p, 4p$ transitions, where the spectral intensity and instrumental resolution allowed us to perform a fit to derive an accurate value of the vibrational spacing, which is found to be 130 meV, in very good agreement with the value 128.1 meV found by Thomas *et al.* for the harmonic symmetric stretching measured in the boron $1s$ photoelectron spectrum [24]. Therefore, we can assign this vibrational progression to the symmetric stretching mode ν_1 .

In this photon-energy range, we detected

- 5 singly charged cations, BF_3^+ , BF_2^+ , BF^+ , B^+ , F^+ ;
- 4 doubly charged cations, BF_2^{++} , BF^{++} , B^{++} , F^{++} ;
- 1 anion, F^- .

No triply charged ions were detected. In figure 2, we show ion yields for the series BF_2^+ , BF^+ , B^+ , F^+ . The yield of the parent ion, BF_3^+ , is very low and shows only a monotonic decrease in this energy range, and thus it is not shown. We observe two main effects for the other singly charged cations. First, the relative intensities of the spectral features related to the Rydberg series increase compared to the B $1s \rightarrow 2a''_2$ transition. This is a trend we have observed in many systems (see for example [20, 21, 22]), and we attribute it to the fact that a core-to-Rydberg excited molecule is more likely to relax via spectator-Auger decay: the excited Rydberg electron is far from the nucleus and the system relaxes preferentially by emitting an electron from an orbital having stronger overlap with the core hole, i.e., a valence orbital, while the initially excited electron remains as a ‘spectator.’ The resulting parent ion is still in an excited state and is energetically more likely to dissociate.

The second observation is that the intensity of the continuum shape resonance varies significantly for the singly charged cations. In particular, it is rather high for the BF^+ and F^+ species. Such intensity enhancement is usually observed instead in the yield curves of doubly charged cations, because the shape resonance leads to core-electron photoionization with subsequent Auger decay, primarily enhancing production of ions with two valence holes. We show the partial yields of the doubly charged cations in figure 3. As expected after normal Auger decay, the doubly charged fragments, except for BF_2^{++} , show increased yield above threshold and enhancement at the shape resonance.

We interpret the lower intensity in the BF_2^{++} fragment as due to fast fragmentation yielding BF^+ and F^+ , resulting in the enhanced production of these singly charged fragments at the shape resonance seen in figure 2.

In figure 4, we show the yield curve for the anion F^- , along with the F^+ yield for comparison. The main characteristic of the anion yield is that the shape resonance has much less intensity compared to the corresponding cation, but it is observed nonetheless. For small systems, diatomic and triatomic molecules (CO [17], CO_2 [25], NO [26], OCS, [27], N_2O [28]), production of anions at a shape resonance is almost completely suppressed, while for larger systems (SF_6 [29, 30], SiF_4 [31], $SiCl_4$ [32]), only a decrease compared to the positive ion counterpart has been observed. The difference between smaller and larger molecular systems is the possibility for large systems to dissipate multiple positive charges over several channels. BF_3 is the first tetra-atomic molecule we have investigated with anion-yield spectroscopy, and the signature of the shape resonance is visible in the anion yield, so we can conclude that four atoms is enough to disperse three positive charges in a fragmentation process and produce anions from normal-Auger final states. Furthermore, neutral doubly excited states have not been observed in BF_3 , but those could exist and overlap with the shape resonance, providing some of the anion intensity.

3.2. F K edge

In figure 5 we show the total ion yield in the photon-energy range 681-715 eV, including the F 1s ionization threshold at 694.8 eV. The photon-energy calibration is based on [1]. The literature assignment [1, 4] indicates the peak at 689.7 eV is the F $1s(a'_1) \rightarrow 2a''_2$ transition, while the peak at 692.55 eV corresponds to the F $1s(a'_1, 1e') \rightarrow 3p$ transition. Above threshold, a broad continuum structure corresponds to two shape resonances of $a1'$ and e' symmetry [1]. We detect all the same cations and anions at the F K edge as seen at the B K edge, plus F_2^+ .

In figure 6 we show yields for the singly charged cations BF_2^+ , BF^+ , B^+ , and F^+ . We observe similar trends to those described for the B K edge. A significant exception is the behavior of the B^+ yield: it does not show relative enhancement of the Rydberg transitions compared to the larger fragments, but rather a high intensity at the F $1s(a'_1) \rightarrow 2a''_2$ transition. This is notably in contrast to the yield of the F^+ fragment. The $2a''_2$ orbital has mainly B $2p_z$ character and is nonbonding in nature. Thus, the enhancement in the B^+ yield could be an indication that B^+ is produced by direct fragmentation of singly charged BF_3^+ into B^+ and three neutral F atoms rather than by Coulomb explosion of a multiply charged species. Why the charge would localize on the B atom following F 1s excitation remains to be explained.

In figure 7 we show partial ion yields for the doubly charged cations. Any trend is difficult to identify, apart from the common characteristics of a high intensity in the region of the shape resonance, which can be explained by the enhanced intensity of the normal Auger decay leading to doubly charged cations.

In figure 8 we show the yield of the anion F^- , together with the total ion yield (TIY) for comparison. We notice some residual intensity above threshold in the shape-resonance region, which was explained in the previous section for the B $1s$ threshold region. There also are pronounced differences for these yields in the Rydberg region and across the ionization threshold. We note that the Rydberg region is much more prominent in the anion yield. We have reported this effect in other systems [33] and attributed it to unstable final states reached after spectator decay which fragment easily and produce anions as well as cations. The other major difference is the behavior at threshold. In the F^+ and all cation yields we notice an increase just above threshold, while in the F^- yield there is an exponential decrease. Such an effect has been observed in CO [18], CO₂ [25], and formic acid [19] and is explained as a post-collision interaction (PCI) effect: above the ionization threshold, the possibility of Auger decay opens up, and formation of anions from the doubly charged final-state ion after Auger decay is unlikely. Just above the edge, there is a possibility the slow photoelectron can be recaptured by the ion after being passed by the fast Auger electron. In a semi-classical description of PCI, the probability for recapture will fall off in a quasi-exponential fashion as the photoelectron kinetic energy increases [34, 35]. Our anion-yield spectrum shows an exponential decrease in anion production above the F $1s$ edge, consistent with a picture where Auger decay makes anion production impossible, but recapture allows it.

3.3. Formation of F_2^+

We show in figure 9 the yield for F_2^+ compared to the yield for B^+ . Formation of F_2^+ requires rearrangement of the molecular structure and involves breaking of two B–F bonds and formation of a new bond between the two fluorine atoms. Examples of intramolecular atomic rearrangement following core excitation are numerous in cases where a hydrogen atom is involved. Breaking of an H–X bond and formation of another bond during photofragmentation is likely due to the high mobility of the proton, and such processes have been observed in several systems: formation of H_2^+ from H_2O [36]; H_2^+ , H_3^+ and HCl^+ from CH_3Cl [21]; and H_2^+ , H_2O^+ , and CH_2^+ from formic acid [19]. Rearrangements involving heavier atoms are more surprising, although we have reported recently the formation of O_2^+ after C $1s$ core excitation in formic acid [19], and N_2^+ after C $1s$ core excitation in cyanogen [33]. In all these examples, intramolecular rearrangement was shown to be helped by vibrational excitation and resonant processes. The same trend is present here, and enhancement at the resonant features is observed in the F_2^+ partial ion yield, although F_2^+ is still observed above threshold, especially at the shape resonance. The experimental resolution combined to the lifetime width of the F $1s$ core-excited state (~ 200 meV) does not allow us to observe any evidence of the role of vibrational excitation in this process, unlike in the case of F_2^+ formation after core excitation in CF_4 as observed at both the C and F K edges [37]. Nonetheless, we can speculate that such a structural change in the molecule is helped by reconfiguration of the electronic structure and subsequent geometrical deformation of the molecule induced

by core excitation. Shimizu et al. have shown that at the F $1a'_1 \rightarrow 2a''_2$ excitation, energetic B^+ ions are ejected in an out-of-plane direction [38]. It was explained by out-of-plane nuclear motion of the B atom, with ion ejection along the remaining B–F bond while two F atoms are released with zero kinetic energy. These two F atoms can then recombine to form F_2^+ . This is supported by the observation that the relative intensity distribution in the F_2^+ partial yield follows closely the B^+ yield (superimposed, the two curves are indistinguishable). We further speculate that formation of F_2^+ is made possible through the same molecular conformational change that leads to the ejection of B^+ . Finally, we note F_2^+ was not detected at the B K edge of BF_3 .

4. Conclusion

Adding to systematic studies of partial cation and anion yields for about 20 molecules, we have recorded partial-ion-yield spectra following core photoexcitation of the BF_3 molecule around the B and F K edges. High detection efficiency measurements for 11 different fragment ions, including singly charged and doubly charged cations and one anion, were presented. No triply charged ions were observed. We also observed the formation of F_2^+ at the fluorine edge. Such ion formation is surprising because it involves intramolecular atomic rearrangement involving heavy atoms, contrary to well-documented cases of hydrogen bond rearrangement in molecules following core excitation.

Acknowledgments

The authors thank the staff of the ALS for their excellent support. Support from the National Science Foundation under NSF Grant No. PHY-05-55699 is gratefully acknowledged. This work was performed at the Advanced Light Source, which is supported by DOE (DE-AC03-76SF00098).

References

- [1] Swanson J R, Dill D, and Dehmer J L 1981 *J. Chem. Phys.* **75** 619, and references therein
- [2] Ishiguro E, Iwata S, Suzuki T, Mikuni A and Sasaki T 1982 *J. Phys. B: At. Mol. Phys.* **15** 1841
- [3] Ueda K, De Fanis A, Saito N, Machida M, Kubozuka K, Chiba H, Muramatu Y, Sato Y, Czasch A, Jaguzki O, Dörner R, Cassimi A, Kitajima M, Furuta T, Tanaka H, Sorensen S L, Okada K, Tanimoto S, Ikejiri K, Tamenori Y, Ohashi H and Koyano I 2003 *Chem. Phys.* **289** 135
- [4] Nekipelov S V, Akomov N N, and Vinogradov A S 1988 *Opt. Spectrosc.* **64** 487
- [5] Miron C, Feifel R, Björneholm O, Svensson S, Naves de Brito A, Sorensen S L, Piancastelli M N, Simon M and Morin P 2002 *Chem. Phys. Lett.* **359** 48, and references therein
- [6] Kanamori H, Iwata S, Mikuni A and Sasaki T 1984 *J. Phys. B: At. Mol. Phys.* **17** 3887
- [7] Ueda K, Chiba H, Sato Y, Hayaishi T, Shigemasa E and Yagishita A 1994 *J. Chem. Phys.* **101** 3520
- [8] Simon M, Miron C, Leclercq N, Morin P, Ueda K, Y Sato, Tanaka S and Kayanuma Y 1997 *Phys. Rev. Lett.* **79** 3857
- [9] Ueda K, Chiba H, Sato Y, Hayaishi T, Shigemasa E and Yagishita A 1992 *Phys. Rev. A* **46** R5

- [10] Ueda K, Ohmori K, Okunishi M, Chiba H, Shimizu Y, Sato Y, Hayaishi T, Shigemasa E and Yagishita A 1995 *Phys. Rev. A* **52** R1815
- [11] Simon M, Morin P, Lablanquie P, Lavollée M, Ueda K and Kosugi N 1995 *Chem. Phys. Lett.* **238** 42
- [12] Ueda K, Ohmori K, Okunishi M, Chiba H, Shimizu Y, Sato Y, Hayaishi T, Shigemasa E and Yagishita A 1996 *J. Electron Spectrosc. Relat. Phenom.* **79** 411
- [13] Tanaka S, Kayanuma Y and Ueda K 1998 *Phys. Rev. A* **57** 3437
- [14] Piancastelli M N 1999 *J. Electron Spectrosc. Relat. Phenom.* **100** 167, and references therein
- [15] Morin P, Simon M, Miron C, Leclercq N, Kukk E, Bozek J D and Berrah N 2000 *Phys. Rev. A* **61** 050701
- [16] Miron C, Simon M, Morin P, Nanbu S, Kosugi N, Sorensen S L, Naves de Brito A, Piancastelli M N, Björneholm O, Feifel R, Bässler M, Svensson S 2001 *J. Chem. Phys.* **115** 864
- [17] Stolte W C, Hansen D L, Piancastelli M N, Dominguez-Lopez I, Rizvi A, Hemmers O, Wang H, Schlachter A S, Lubell M S and Lindle D W 2001 *Phys. Rev. Lett.* **86** 4504
- [18] Hansen D L, Stolte W C, Hemmers O, Guillemin R, and Lindle D W 2002 *J. Phys. B: At. Mol. Opt. Phys.* **35** L381
- [19] Guillemin R, Stolte W C, and Lindle D W 2009 *J. Phys. B: At. Mol. Opt. Phys.* **42** 125101
- [20] Piancastelli M N, Stolte W C, Öhrwall G, Yu S -W, Bull D, Lantz K, Schlachter A S and Lindle D W 2002 *J. Chem. Phys.* **117** 8264
- [21] Céolin D, Piancastelli M N, Guillemin R, Stolte W C, Yu S -W, Hemmers O, and Lindle D W 2007 *J. Chem. Phys.* **126** 084309
- [22] Céolin D, Piancastelli M N, Stolte W C and Lindle D W 2009 *J. Chem. Phys.* **131** 244301
- [23] Stolte W C, Guillemin R, Yu S -W, and Lindle D W 2008 *J. Phys. B: At. Mol. Opt. Phys.* **41** 145102
- [24] Thomas T D, Püttner R, Fukuzawa H, Prümper G, Ueda K, Kukk E, Sankari R, Harries J, Tamenori Y, Tanaka, T, Hoshino M, and Tanaka H 2007 *J. Chem. Phys.* **127** 244309
- [25] Öhrwall G, Sant'Anna M M, Stolte W C, Dominguez-Lopez I, Dang L T N, Schlachter A S and Lindle D W 2002 *J. Phys. B: At. Mol. Opt. Phys.* **35** 4543
- [26] Yu S -W, Stolte W C, Öhrwall G, Guillemin R, Piancastelli M N, and Lindle D W 2003 *J. Phys. B: At. Mol. Opt. Phys.* **36** 1255
- [27] Dang L T N, Stolte W C, Öhrwall, Sant'Anna M M, Dominguez-Lopez I, Schlachter A S and Lindle D W 2003 *Chem. Phys.* **289** 45
- [28] Yu S -W, Stolte W C, Guillemin R, Öhrwall G, Tran I C, Piancastelli M N, Feng R and Lindle D W 2004 *J. Phys. B: At. Mol. Opt. Phys.* **37** 3583
- [29] Scully S W J, Mackie R A, Browning R, Dunn K F and Latimer C J 2002 *J. Phys. B* **35** 2703
- [30] Piancastelli M N, Stolte W C, Guillemin R, Wolska A, Yu S -W, Sant'Anna M M, and Lindle D W 2005 *J. Chem. Phys.* **122** 094312
- [31] Piancastelli M N, Stolte W C, Guillemin R, Wolska A, and Lindle D W 2008 *J. Chem. Phys.* **128** 134309
- [32] Chen J M, Lu K T, Lee J M, Chou T L, Chen H C, Chen S A, Haw S C and Chen T H 2008 *New J. Phys.* **10** 103010
- [33] Öhrwall G, Stolte W C, Guillemin R, Yu S -W, and Lindle D W 2010 *J. Phys. B : At. Mol. Opt. Phys* **43** 095201
- [34] Eberhardt W, Bernstorff S, Jochims H W, Whitfield S B, and Crasemann B 1988 *Phys. Rev. A* **38** 3808
- [35] Armen G B and Levin J C 1997 *Phys. Rev. A* **56** 3734
- [36] Piancastelli M N, Hempelmann A, Heiser F, Gessner O, Rüdell A, and Becker U 1999 *Phys. Rev. A* **59** 300
- [37] Guillemin R et al, to be published
- [38] Shimizu Y, Ueda K, Chiba H, Okunishi M, Ohmori K, West J B, Sato Y, and Hayaishi T 1997 *J. Chem. Phys.* **107** 2419

FIGURE CAPTIONS

- Fig. 1: Total ion yield in the photon-energy range 193-212 eV, including the B 1s ionization threshold at 202.8 eV. Calibration and spectral assignments from [2]. The insert shows a fit of the 199.5–202.5 eV region around the 3*p* and 4*p* Rydberg states (see text).
- Fig. 2: Partial ion yields for the singly charged cations BF₂⁺, BF⁺, B⁺, F⁺ in the photon-energy range 190-212 eV.
- Fig. 3: Partial ion yields for the doubly charged cations BF₂⁺⁺, BF⁺⁺, B⁺⁺, F⁺⁺ in the photon-energy range 190-212 eV.
- Fig. 4: Partial ion yields for F⁺ and F⁻ in the photon-energy range 190-212 eV.
- Fig. 5: Total ion yield in the photon-energy range 683-713 eV, including the F 1s ionization threshold at 694.8 eV. Calibration and spectral assignments from [1].
- Fig. 6: Partial ion yields for the singly charged cations BF₂⁺, BF⁺, B⁺, and F⁺ in the photon-energy range 683-713 eV around the F 1s ionization threshold.
- Fig. 7: Partial ion yields for the doubly charged cations BF₂⁺⁺, BF⁺⁺, B⁺⁺, and F⁺⁺ in the photon-energy range 683-713 eV around the F 1s ionization threshold.
- Fig. 8: Total ion yield (TIY) and F⁻ partial ion yield in the photon-energy range 681-716 eV around the F 1s ionization threshold, indicated by the vertical line.
- Fig. 9: Partial yield for F₂⁺ compared to the partial yield for B⁺ in the photon-energy range 681-716 eV around the F 1s ionization threshold.

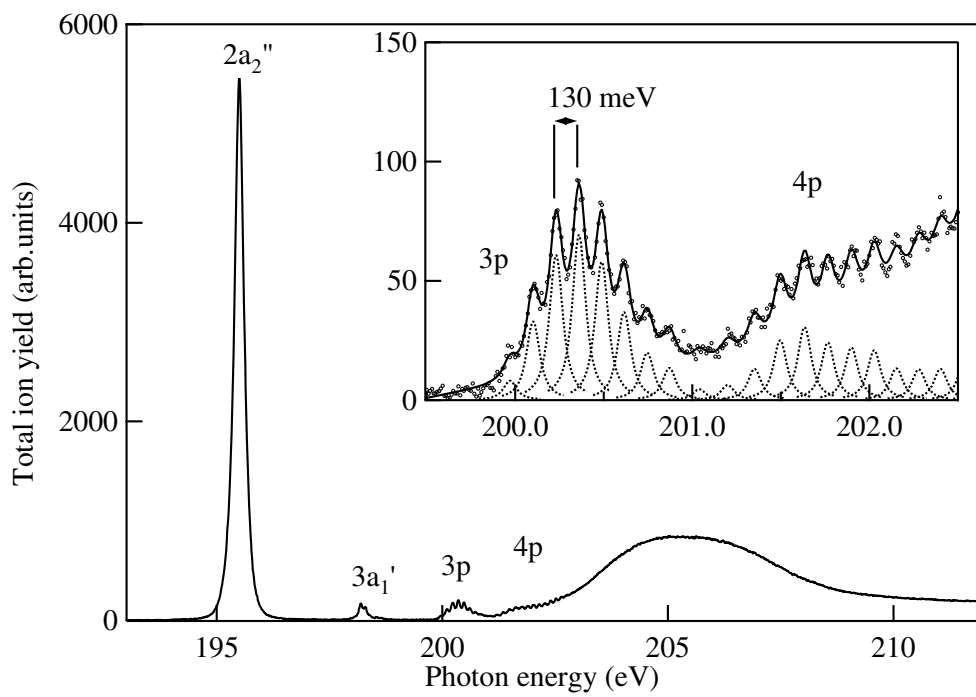


Figure 1.

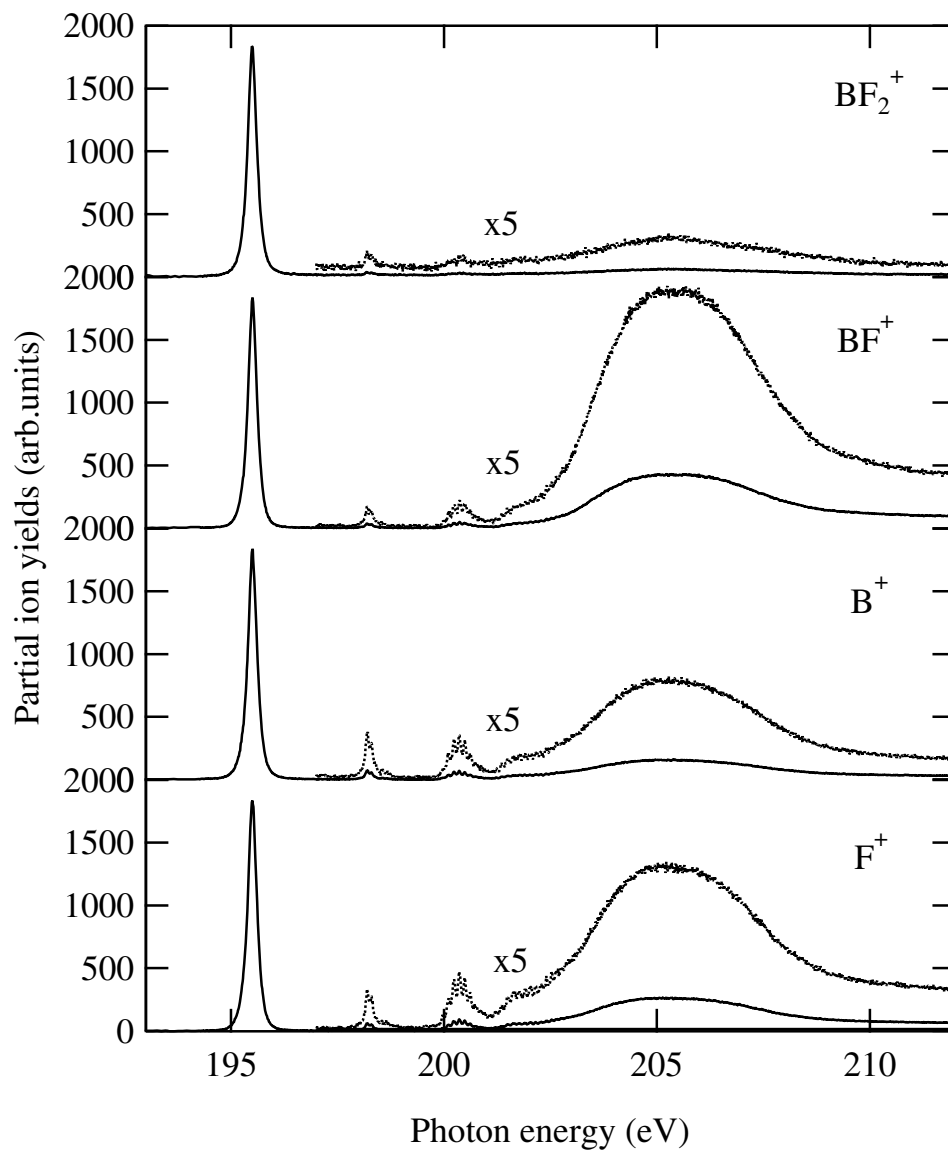


Figure 2.

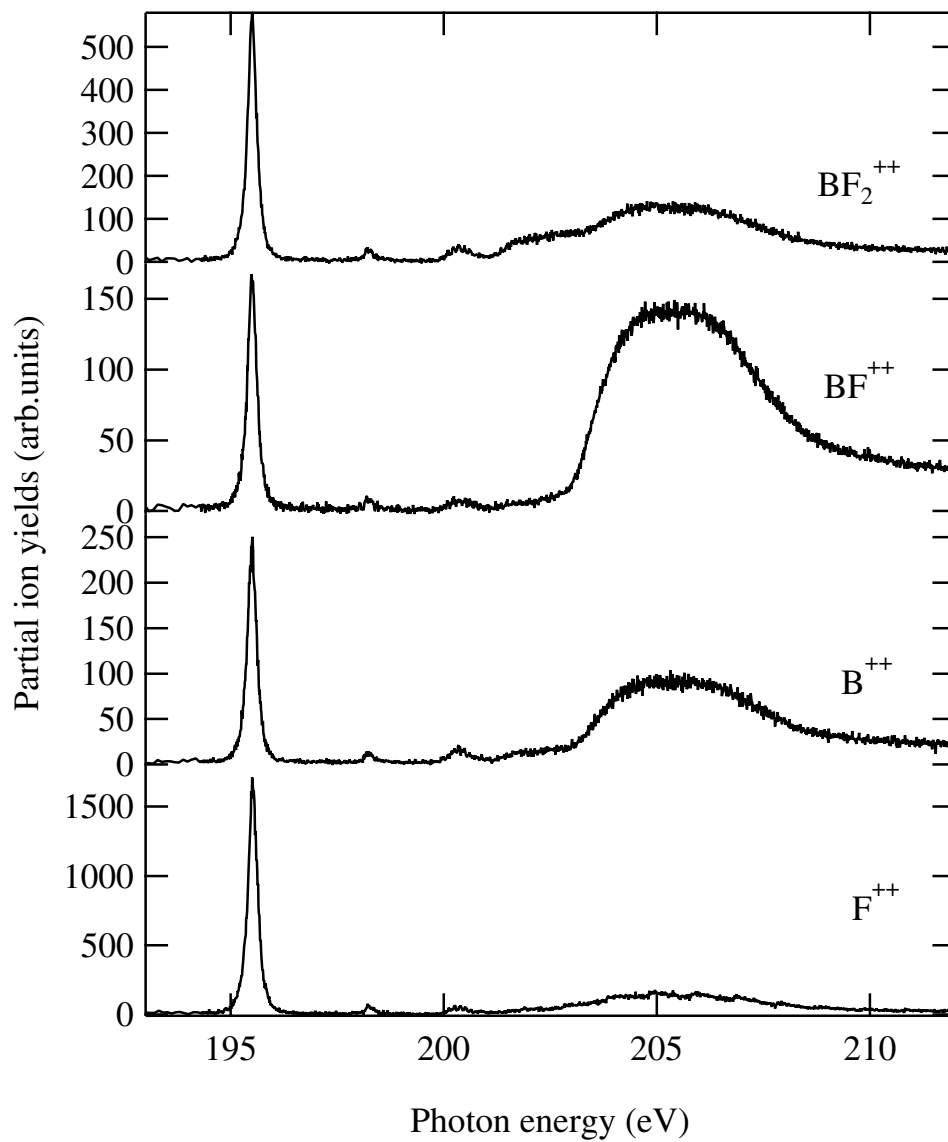


Figure 3.

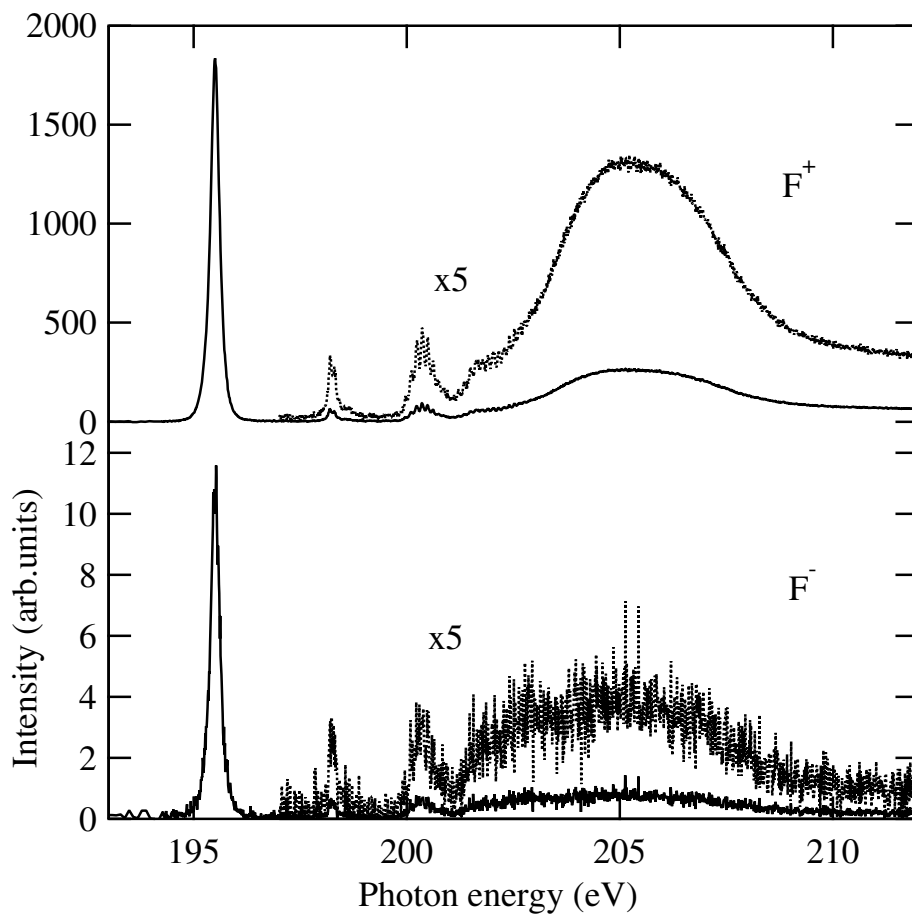


Figure 4.

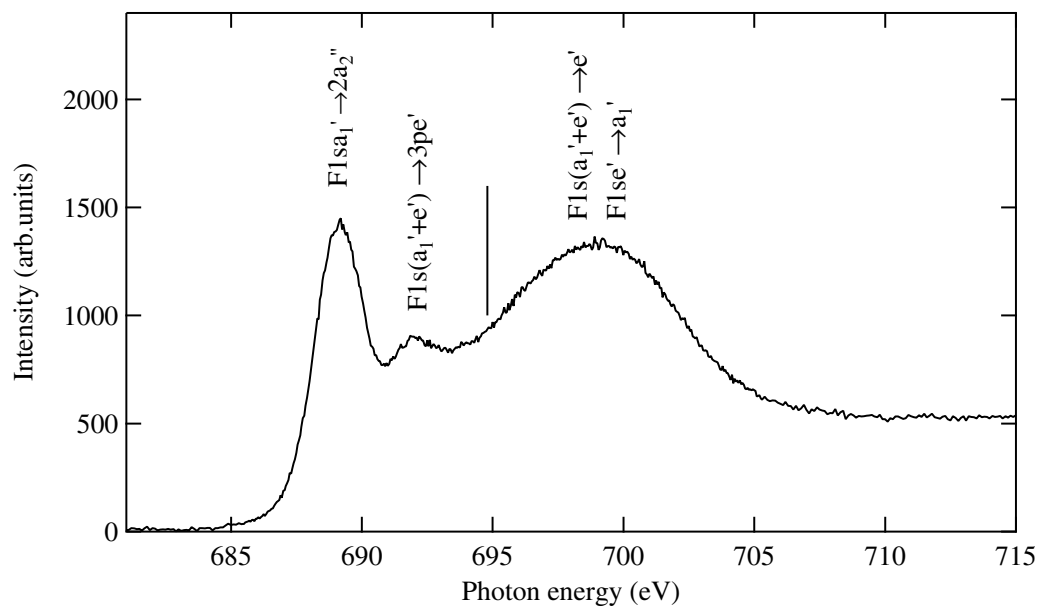


Figure 5.

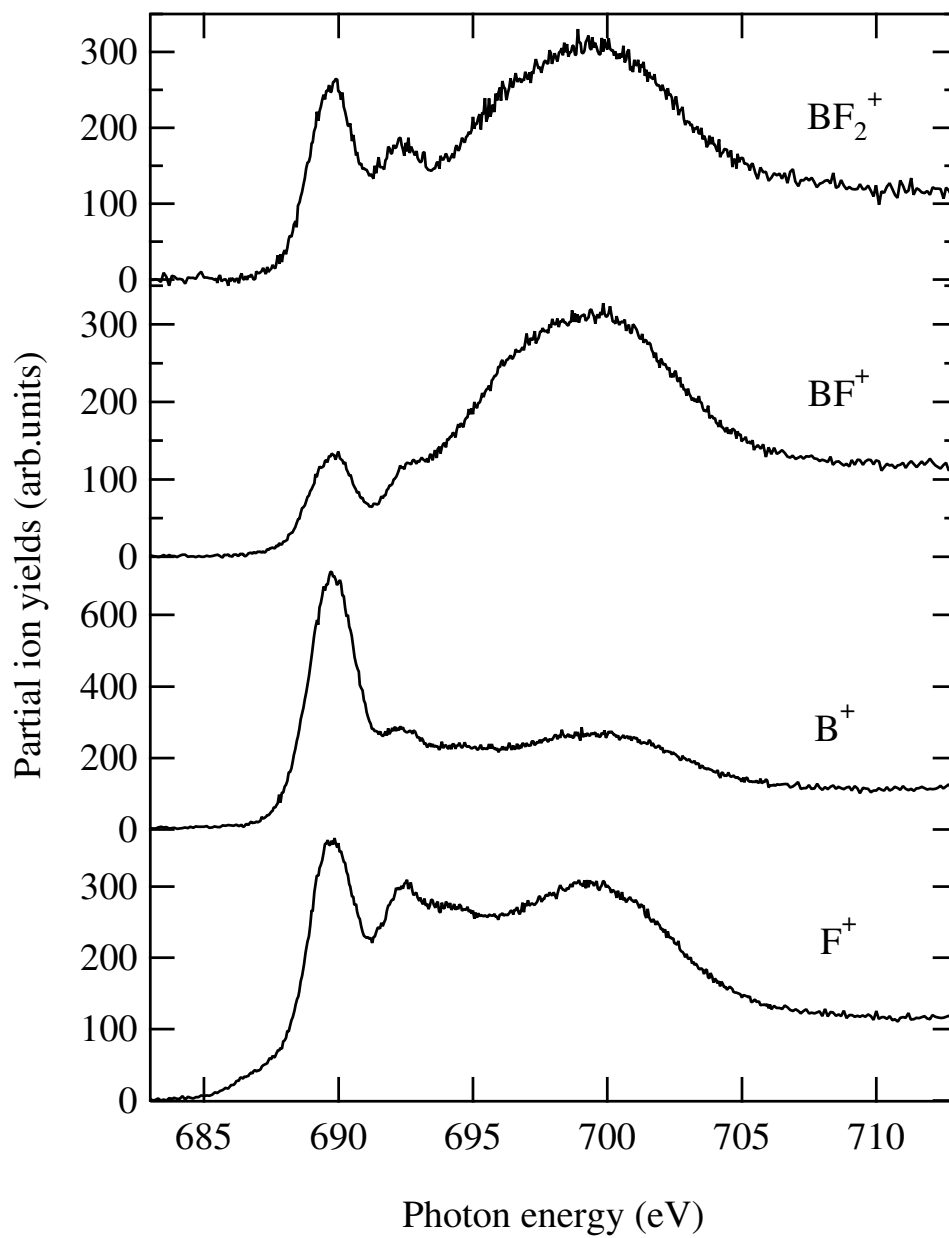


Figure 6.

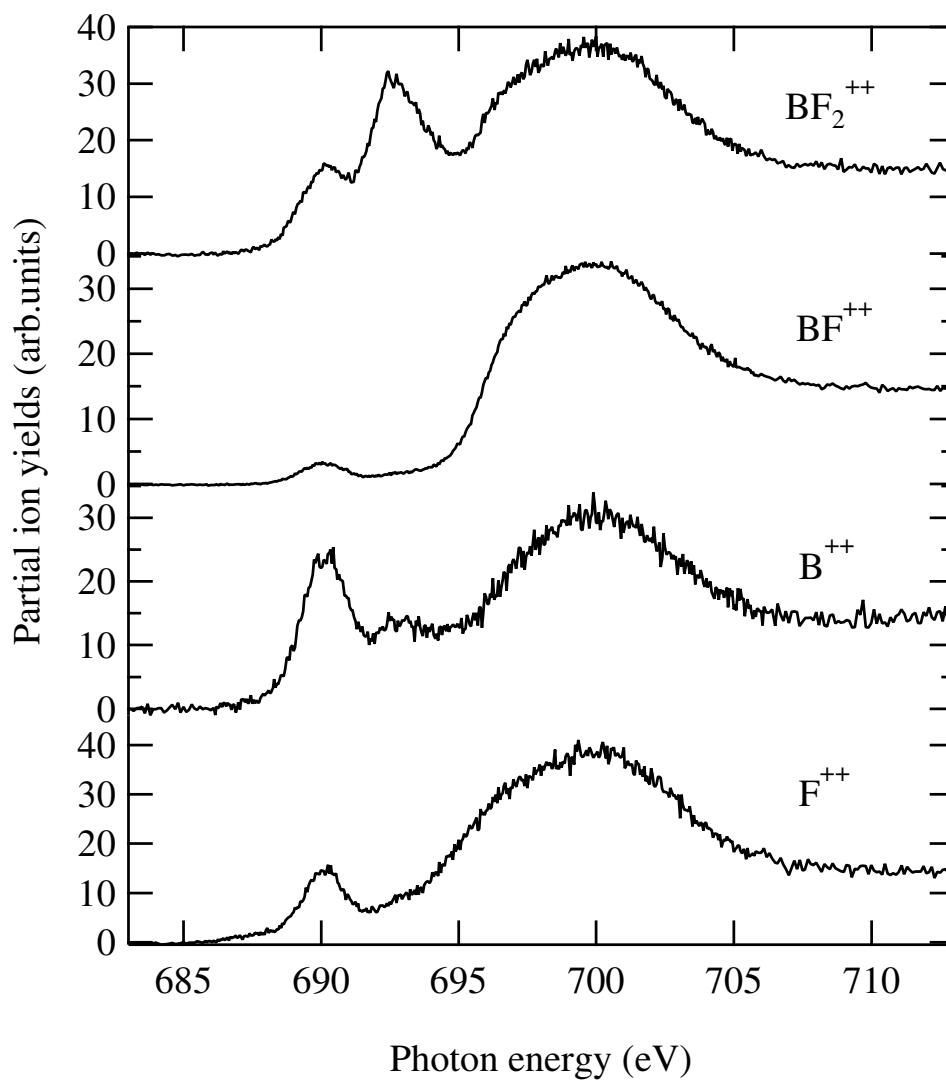


Figure 7.

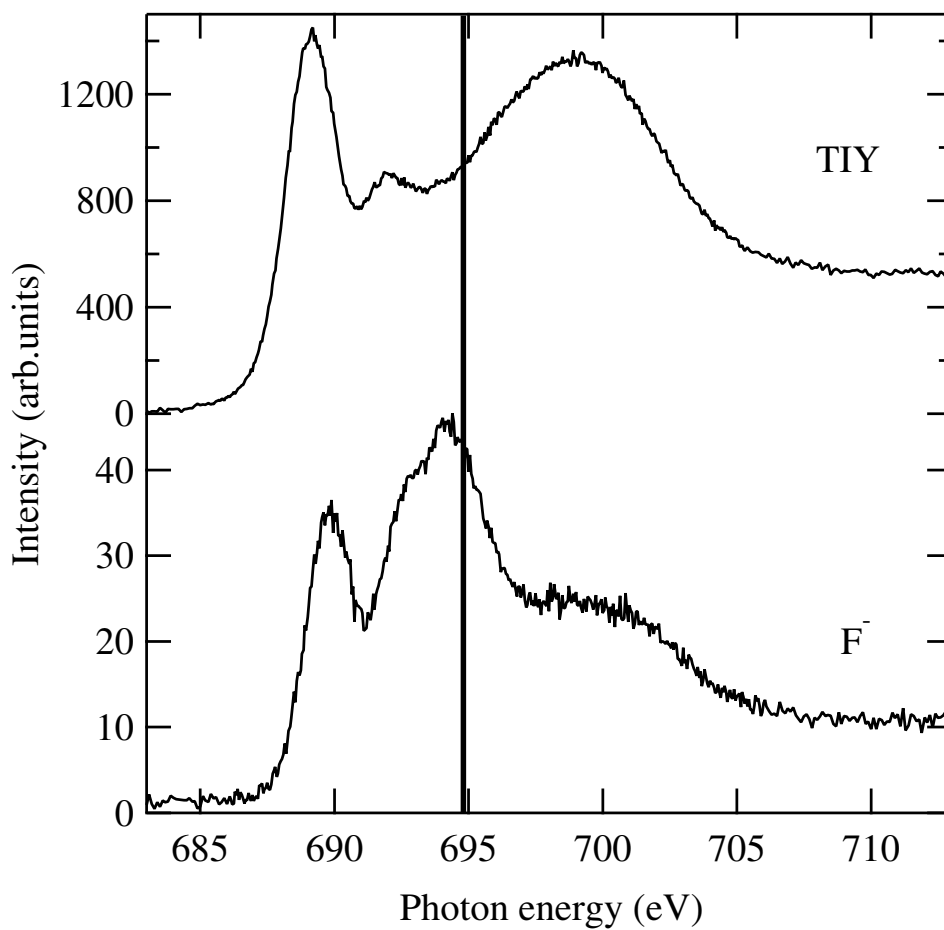


Figure 8.

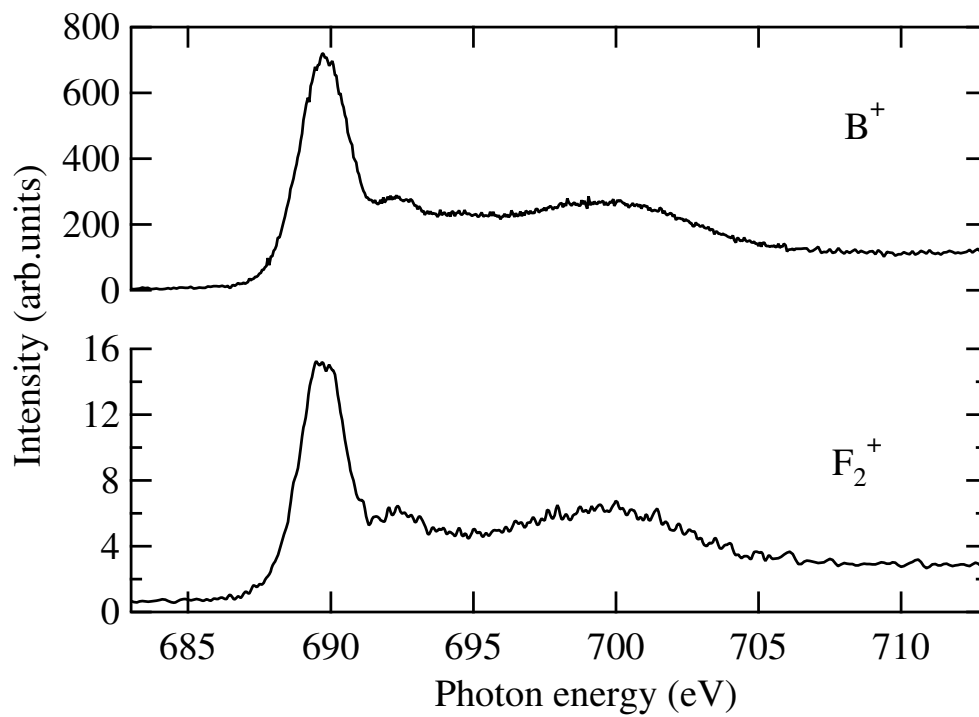


Figure 9.